Journal of X-Ray Science and Technology 31 (2023) 211–221
DOI 10.3233/XST-221301
IOS Press

Lung cancer histopathological image classification using wavelets and AlexNet

Prabira Kumar Sethy[a], A. Geetha Devi[b], Bikash Padhan[a], Santi Kumari Behera[c,*], Surampudi Sreedhar[d] and Kalyan Das[e]
[a]*Department of Electronics, Sambalpur University, Jyoti Vihar, Burla, India*
[b]*Department of Electronics and Communication Engineering, PVP Siddhartha Institute of Technology, Vijayawada, AP, India*
[c]*Department of Computer Science and Engineering, VSSUT, Burla, India*
[d]*Aware College of Medical Lab Technology, Bairamalguda, Hyderabad, India*
[e]*Department Computer Science Engineering and Application, Sambalpur University Institute of Information Technology, Burla, India*

Received 12 September 2022
Revised 20 October 2022
Accepted 12 November 2022

Abstract. Among malignant tumors, lung cancer has the highest morbidity and fatality rates worldwide. Screening for lung cancer has been investigated for decades in order to reduce mortality rates of lung cancer patients, and treatment options have improved dramatically in recent years. Pathologists utilize various techniques to determine the stage, type, and subtype of lung cancers, but one of the most common is a visual assessment of histopathology slides. The most common subtypes of lung cancer are adenocarcinoma and squamous cell carcinoma, lung benign, and distinguishing between them requires visual inspection by a skilled pathologist. The purpose of this article was to develop a hybrid network for the categorization of lung histopathology images, and it did so by combining AlexNet, wavelet, and support vector machines. In this study, we feed the integrated discrete wavelet transform (DWT) coefficients and AlexNet deep features into linear support vector machines (SVMs) for lung nodule sample classification. The LC25000 Lung and colon histopathology image dataset, which contains 5,000 digital histopathology images in three categories of benign (normal cells), adenocarcinoma, and squamous carcinoma cells (both are cancerous cells) is used in this study to train and test SVM classifiers. The study results of using a 10-fold cross-validation method achieve an accuracy of 99.3% and an area under the curve (AUC) of 0.99 in classifying these digital histopathology images of lung nodule samples.

Keywords: Lung cancer, histopathological images, wavelet, AlexNet, support vector machine (SVM), cancer diagnosis

1. Introduction

Cancer is a disease that begins when cells in the body begin to form abnormally and spread throughout the body. Cancer can originate in virtually any organ or tissue of the body. Cancer is the main cause of the second leading cause of death worldwide, and it is estimated to account for 9.6 million fatalities or one out of every six deaths, in 2018 [1]. Compared to colorectal cancer, which accounts for 1.80

*Corresponding author: Santi Kumari Behera, Department of Computer Science and Engineering, VSSUT, Burla-768018, India. E-mail: b.santibehera@gmail.com, https://orcid.org/0000-0003-4857-7821.

ISSN 0895-3996/$35.00

million cases but only 783 thousand fatalities, lung cancer accounts for 2.06 million diagnoses and 1.76 million deaths [1]. This includes both small cell and non-small cell forms of the disease. Small cellular carcinoma in the lungs (also known as SCLC) and non-small cell cancer are the two forms of lung cancer that can emerge from nowhere and quickly spread throughout the body (NSCLC). Small cell lung cancer (SCLC) is a subtype of lung cancer that accounts for 15% of all instances of the disease. It is an extremely hazardous tumor that develops from cells that have neuroendocrine characteristics. The American Joint Committee on Cancer (AJCC) has developed and continues to maintain a staging system known as the Tumor-Node-Metastasis (TNM) system. This method has found that most malignancies may be divided into five distinct stages. The size and location of the main tumor, the amount to which it has progressed to the lymph nodes and other organs, and the existence of any biomarkers that influence the spread of cancer are some of the many parameters that a system needs to take into consideration [1]. The chances of survival at each stage are significantly different from one another.

To classify the cancers, it is required to process the histopathological images. The pathologists will predict the patient's survival rate by studying the histopathological images. These images are obtained from the biopsy (tissue sampling) or a surgical sample which are processed and fixed onto a glass slither. In traditional methods, health experts follow a long procedure to process these images. To overcome this issue, a hybrid network is proposed to classify lung histopathological images, comprising high-level feature extraction techniques and machine learning classifier. Here, the high-level features are extracted using Discrete wavelet transforms (DWT), and those obtained features are combined with deep features obtained from AlexNet. Then, the combination of high-level fused features is fed to linear SVM for classification, and the output classified images are obtained.

The histopathological images contain hyperspectral data. It has discriminative spatial and spectral characteristics. To classify hyperspectral data, there are numerous classifiers available in literature such as support vector machines (SVMs) [2, 3], artificial neural networks (ANN) [4], sparse representation methods [5], random forest (RF) methods [6], and convolution neural network (CNN) [7, 8], etc. The discrete wavelet transform (DWT) represents the images at more than one resolution by discrete sampling, which is very helpful for analyzing the images. Moreover, it provides features at various solutions. For example, the spectral information can be obtained using DWT by applying multispectral image data multi-level decomposition. Especially, the variations in the local spectra are detected at different spectral bands of wavelet transformed images.

The DWT comprises two main blocks namely, (1) the Filter Bank (FB) and (2) the Lifting Scheme (LS). The DWT is a truncated wavelet transform that is half the image size at each scale. In the wavelet transform, converting spatial domain inputs to frequency domain is simple [10]. The input series $y_0, y_1, \ldots, y_n$ are used to generate high pass and low pass coefficient series. The following Equations (1) and (2) are used to represent the high and low pass coefficients, respectively.

$$H_i = \sum^{l-1}(2j - n).(z) \quad n = 0 \tag{1}$$

$$= \sum^{l-1}(2j - n).(z) \quad n = 0 \tag{2}$$

where the wavelet filters are denoted by the letters sn(z) and tn(z), the length of the filter is given by l, and $j = 0,...,$ [n/2]-1.

The spatial domain DWT is employed in two directions. The horizontal axis is first subjected to 1D-DWT, and the results are then applied to the vertical axis. The four sections obtained from the 2D-DWT are LL, LH, HL, and HH. All image's rows and columns are affected by the two-dimensional DWT. For example, the input image size at level $L+1$ will be 2k/2×2k/2 if the input image is 2k×2k

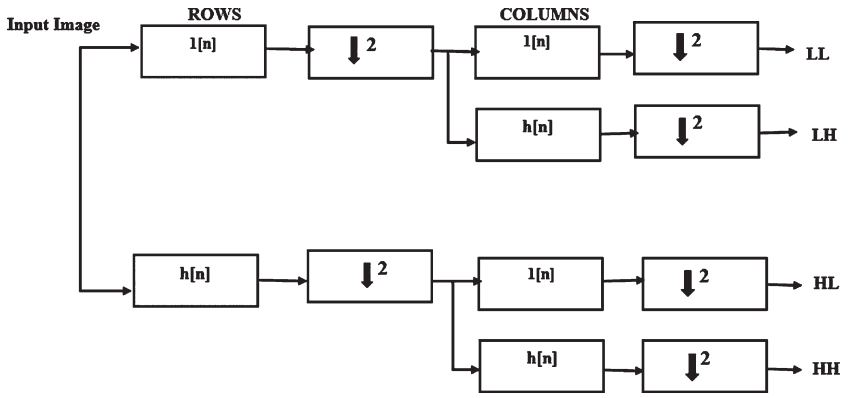

Fig. 1. Discrete wavelet transforms.

pixels in size. Wavelets across an image employ a variety of decomposition algorithms. The DWT is used to break down the input image into four sub-images. Sub-bands are the names given to these smaller images. The coarse level sub-image is represented by the LL sub-band, while the diagonal, vertical, and horizontal components are represented by the HH, LH, and HL sub-bands. The input image is finally split into four major components, as shown in Fig. 1. For multi-resolution analysis, LL frequency and low pass components create a high-level 2D-DWT.

Let's assume the input image is Y. Here, Y is split into two different bands, such as Y_o and Y_e.

$$Y_o = [(1), (3), (5) \ldots (2n-1)] \tag{3}$$

$$Y_e = [(2), (4), (6) \ldots (2n)] \tag{4}$$

$$Q_1(n) = Y_o(n) + a(Y_e(n) + Y_e(n+1)) \tag{5}$$

$$V_1(n) = Y_e(n) + b(Q_1(n) + Y_e(n+1)) \tag{6}$$

$$(n) = L.Q_1(n) \text{ Here, } Q_1(n) \text{ is scaled by } L. \tag{7}$$

Machine learning algorithms can perform tasks such as categorizing and predicting a wide variety of biomedical image types. Learning algorithms are described by Deep Learning (DL) algorithms, which are a subfield of machine learning. These algorithms mimic how the human brain learns using artificial neural networks (ANNs). It makes it possible for machines to process high-dimensional data such as images, videos, and multidimensional anatomical images, among other data types. Above all else, it is obvious that AI has added a new dimension to the field of medical diagnosis, and it is increasingly becoming available as a substitute for conventional diagnostic procedures.

The AlexNet [11] is a popular convolutional neural network (CNN) comprised of 8 layers. In these eight layers, 5 Layers are CNNs followed by Max pooling layers and 2 Layers are Fully connected hidden layers, and one layer is fully connected output layer. The activation function used in Alex Net is ReLU. Multiple GPUs can be used to train the Alex Net. Conventionally, CNN's "pool" outputs of neighboring groups of neurons with no overlapping. Alex Net had 60 million parameters which is a major problem in terms of overfitting, and this can be avoided in two methods.1. Data Augmentation and 2. Dropout. In this paper, data augmentation is taken.

There are many challenges in using AI technologies in the medical sector. Hence, there is more scope for research in this area. The main contribution of this paper is the utilization and combination

of high-level features obtained from DWT & AlexNet to enhance the classification accuracy of SVM for the classification of lung histopathological images.

The major contribution of this article are as follows.

- Extracting the most important high-level deep features by fine-tuning the AlexNet.
- Added a concatenation layer, where the high-level features, i.e., coefficients of DWT, are mixed with the deep features of AlexNet.
- Hybrid model is proposed with consideration of high-level features of AlexNet, DWT and SVM classifier.
- The achieved accuracy is 99.3%, which is outperformed than the state-of-art, irrespective of image modalities.

The remaining paper is organized as follows. The materials and methods section describe the dataset and the proposed methodology using DWT and wavelets. 1) Division of data to perform three binary classification problems. 2) Data augmentation using augmenter software package 3) Feature Extraction using transfer learning through various Pre-trained AlexNet. 4) Evaluation of performances on various metrics. 5) Conclusion and future work.

2. Related works

In 1955, Lee Lusted recognized the use of computers in medical diagnosis [12]. In 1963, Lodwick et al. digitized chest X-rays for the first time to develop Computer-Aided Diagnosis (CAD) applications and applied them to diagnose Lung cancer. Lung cancer identification using chest radiographs was among the most researched CAD applications in the 70 s and 80 s [13]. However, the invention of DL methods has drastically changed the field of medical imaging. Many DL and non-DL methods are available in the literature to classify medical images. But in this paper, the focus is on the classification of Lung cancer images. Hence, we emphasize the methodologies in this area. The methods vary with image modalities, the applied techniques for features extraction, and the design of the ML model used for cancer identification [14]. Shi et al. described a lung cancer Classification using the multi-modal Sparse Representation method. They studied specimens of captured needle biopsy and segmented 4,372 cell nuclei regions for lung cancer classification [15]. The classification accuracy on average of their proposed method reached 88.10%. Kuruvilla and Gunavathi analyzed lung cancer CT scan images and proposed an image classification method [16] in 2014. They classified the image data using two Artificial Neural Networks (ANNs) based on six types of statistical features. The first ANN is with only forward propagation, and the other ANN is with forwarding and backpropagation. It is found that the normalized third-order central moment (skewness), when paired with ANN with backpropagation, provides the best classification outcome.

In the same year, a noninvasive pulmonary nodule diagnosis method was inscribed by Deppen et al. based on the analysis of PET scanned images along with Flu deoxy glucose F-18 (FDG) data [17]. They tested the method on 8511 cases, among which 60% were malignant, and their model detected them with high sensitivity and specificity. “Shen et al. proposed a lung nodule detection and classification scheme using a Multi – crop CNN (MC-CNN) [18]”. This approach has not applied CT scan images with any segmentation or feature extraction techniques. The proposed ML model achieved a classification accuracy of 87.14%. A CNN and Deep Belief Network (DBN) has been developed by Sun et al. and used on 134,668 CT scan images to detect the presence of lung cancer in them [19]. Yuan et al. described a DL method automatically detecting lumps from colonoscopy videos [20]. AlexNet has been used for classification. Alex Net is a well-known CNN-based architecture, and this methodology’s classification accuracy is 91.47%. Selvanambi et al. proposed a Lung cancer

prediction method based on glowworm swarm optimization (GSO) using images from multiple sources in 2018 [21]. A recurrent Neural Network (RNN) has been utilized as the learning algorithm, and a maximum of 98% accuracy is obtained. De Carvalho Filho et al. proposed a lung cancer identification based on CNN. They tested the network on a dataset containing over 50,500 CT scan images [22]. In addition, Da Nóbrega et al. described a method using ResNet50 and CNN to identify the malignant nodule in the lung. Their study also explored other learning methods like Transfer Learning, ImageNet, MobileNet, Xception, and InceptionV3 [23]. Mostly, authors are working on deep learning for lung cancer diagnosis [24–28], recently.

3. Material and methods

3.1. Image dataset

The data is extracted from the LC25000 Lung and colon histopathology image dataset, which contains 5,000 images in three classifications of benign (normal cells), adenocarcinoma, and squamous carcinoma cells (both are cancerous cells). The number of original images received is only 750; their dimensions are 1024×768 pixels, with 250 images allocated to each category. These images are

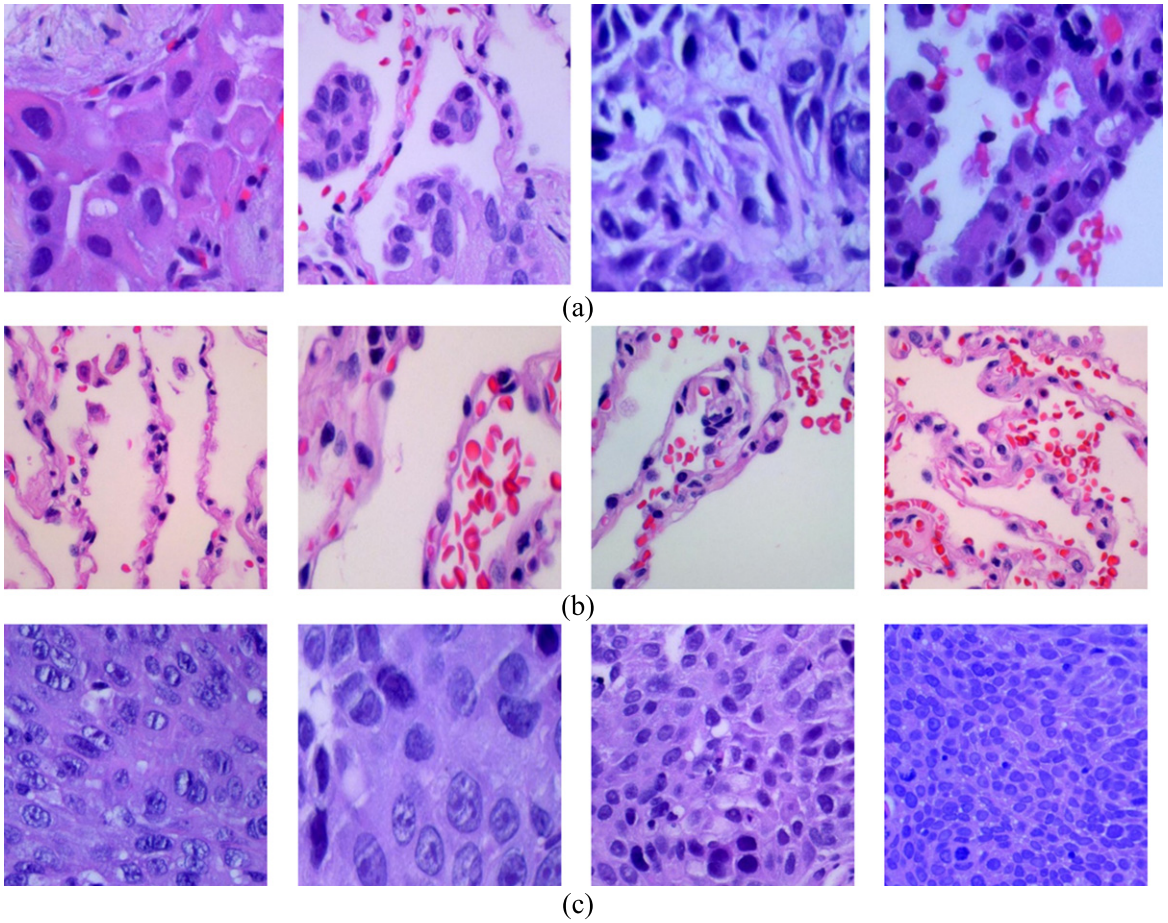

Fig. 2. Sample images of three classes present in the dataset. (a) lung_aca (lung adenocarcinoma tissue), (b) lung_n (lung benign tissue), and (c) lung_scc (lung squamous cell carcinoma tissue).

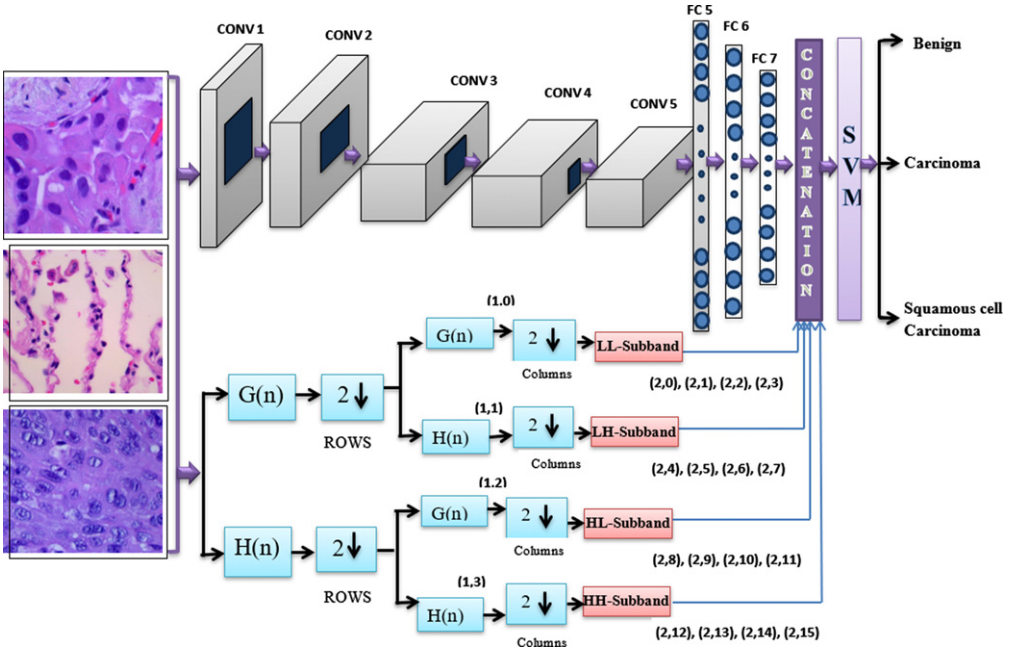

Fig. 3. Proposed methodology for classification of breast cancer histopathological images.

cropped to 768×768 pixels before being augmented. Consequently, the increased dataset includes 5,000 images in each category. The horizontal and vertical flips and the left and right rotations are used for augmentation. Figure 2 depicts examples of photographs within each category.

3.2. Proposed methodology

The proposed classification framework uses spectral coefficients of DWT multi-level decomposition followed by spatial filtering of all LL, LH, HL, and HH coefficients for each level of decomposition. Thus, in our proposed approaches, we perform a spectral DWT multi-level decomposition on the original dataset, and it is then concatenated with the features obtained from the AlexNet. In addition, a Linear SVM machine has been utilized to classify the histopathological images of Lung cancers. The proposed methodology is illustrated in Fig. 3.

Due to protection and privacy considerations, there are extremely few clinical field datasets [29]. Histological images, on the other hand, are incredibly unpredictable. Therefore, creating a model without any preparation from scratch with randomly initialized features with low data measurements would be difficult and troublesome. This study employs pre-trained CNN models like AlexNet to address these problems. The goal is to apply the weights from an existing model to different issues. Transfer learning is another name for this method [30]. It helps to reduce the computational load and speed up system performance, leading to quicker and better outcomes. Thus, we suggest a structure in this study that could be used for a three-way categorization challenge. There are three divisions in the structure:

i. Feature Extraction Part - Extracting the most important high-level deep features by fine-tuning the AlexNet.
ii. Modified Part - Added a concatenation layer, where the high-level features, i.e., coefficients of DWT, are mixed with the deep features of AlexNet.

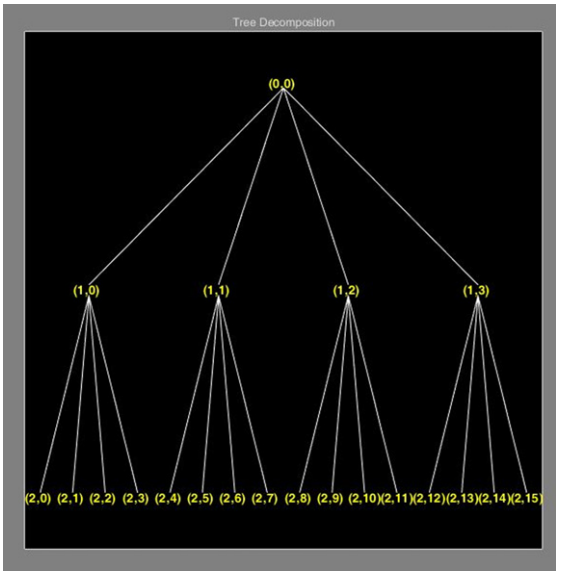

Fig. 4. DWT tree decomposition.

iii. Classification – The SVM performs the classification task by utilization of enhanced high-level features (deep features+DWT coefficients).

In 2D-DWT, the image is decomposed into high-frequency (details) and low-frequency components (approximation). At every level, four sub-bands are generated. The approximation shows an overall trend of pixel values and the details as the horizontal, vertical, and diagonal components. As, 2 level decomposition is carried out, a total of 20 coefficients (16 coefficients of 2nd level and four coefficients 1st level) are generated [24]. The decomposition tree is illustrated in Fig. 4.

Thus, in above DWT tree decomposition structure, the four coefficients in the 1st level, such as (1,0), (1,1), (1,2), and (1,3) are generated. Again, in the 2nd level 16 coefficients such as (2,0), (2,1), (2,2), (2,3), (2,4), (2,5), (2,6), (2,7), (2,8), (2,9), (2,10), (2,11), (2,12), (2,13), (2,14) and (2,15) are generated. These 20 coefficients are added to the 1094 number of deep features generated by AlexNet. Thus, a total of 1110 (1094 + 20) features are fed to the linear SVM classifier.

4. Result and discussion

This section presents the proposed method's acquired results, and other machine learning models are investigated in the same dataset. Indeed, the models were evaluated on the test data to determine their performance. The proposed model was built on an Intel(R) Core (TM) i7-12th generation processor using MATLAB 2021a. A graphical processing unit (GPU) NVIDIA RTX 3050 Ti with 4 GB and 16 GB RAM was also used to run the experiments. The performances of all models are evaluated using 10-fold cross-validation techniques. The confusion matrix and AUC are illustrated in Fig. 5. Furthermore, the computed TPR, FNR, PPV, and FDR of the proposed methodology are recorded in Table 1.

In order to compare our model with existing models in the literature, several other machine learning models are executed using the same dataset with 10-fold cross-validation. Results of the classification accuracy of these machine learning models are reported and compared in Table 2. Three sets of features are fed into four typical classifiers in this case. The comparison result showed that the LBP feature with

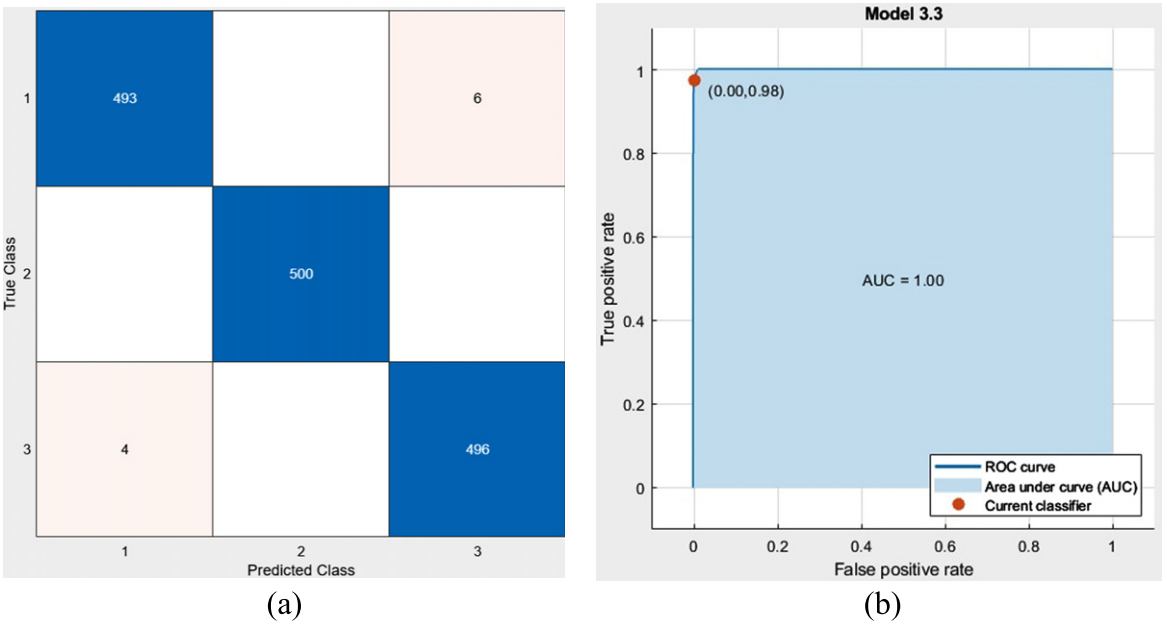

Fig. 5. Performance of proposed method (a) confusion matrix (b) AUC *(*Indices 1: lung_aca, 2: lung_n, 3: lung_scc).*

Table 1
TPR, FNR, PPV, and FDR of the proposed model for lung cancer histopathological image classification

Class	TPR (%)	FNR (%)	PPV (%)	FDR (%)
lung_aca	98.8	1.2	99.2	0.8
lung_n	100.0	0.0	100	0.0
lung_scc	99.2	0.8	98.8	1.2

Table 2
Performance measures in accuracy (%) with different machine learning strategies

	SVM	RF	LDA	MLP
GLCM	90.0	86.8	87.4	90.4
LBP	95.1	94.1	90.3	91.2
HOG	89.0	88.1	80.4	83.2

SVM outperformed other machine learning models or techniques with an accuracy of 95.1%. Although there is still room for improvement, it can be concluded that ML models, particularly the LBP+SVM model, are quite accurate in classifying subtypes of lung cancer. In the most current study articles, the authors used deep learning to categorize histological images of lung tumors. Table 3 compares our findings utilizing the same dataset and those from published studies.

Indeed, most of the previous studies used deep learning. In contrast, our study used a hybrid model where the coefficients of 2D-DWT are added with deep features extracted from AlexNet and the enhanced feature set fed to SVM for classification of lung histopathological images. It is observed from Table 3 the proposed method outperformed the previous method irrespective of image modalities. For more clarification about the contribution of coefficients of 2D-DWT, we executed the same

Table 3
Comparison of results with state-of-art

Reference	Image Types	Classifiers	Accuracy (%)
[31]#	Histopathological	CNN	97.2
[32]#	Histopathological	CNN	97.8
[33]	Biopsy image	MSRP	88.1
[34]	CT scan	ANN	93.3
[18]	CT scan	MC-CNN	87.14
[19]	CT scan	CNN	89.9
[22]	CT scan	CNN	92.63
[23]	CT scan	RestNet50 + SVM RBF	93.19
[35]	CT scan	DFCNet	89.52
[36]	CT scan	DAELGNN	99.65
[37]	CT scan	CNN	93.9
[38]	CT scan	CNN	97.9
[39]	CT scan	EM	96.2
Proposed model#	Histopathological	Alexnet+DWT+SVM	99.3

#Works with the same dataset of LC25000 dataset.

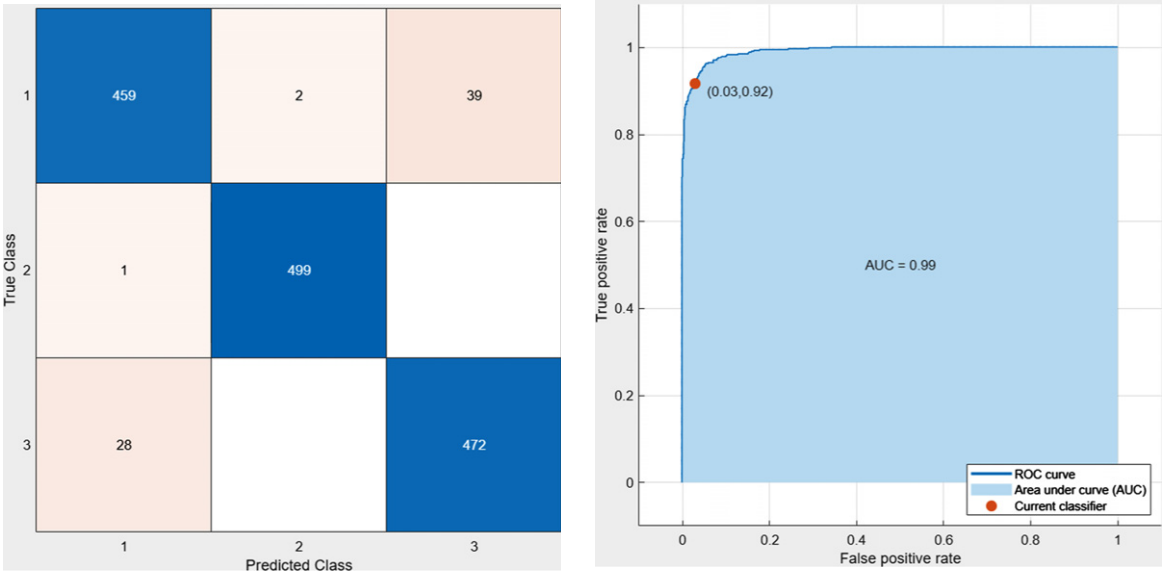

(a) (b)

Fig. 6. Performance of AlexNet+SVM without the addition of DWT coefficients (a) confusion matrix (b) AUC. (*Indices 1: lung_aca, 2: lung_n, 3: lung_scc).

model (AlexNet+SVM) with the same dataset with the same evaluation strategy without adding DWT coefficients. The confusion matrix and AUC are illustrated in Fig. 6.

The model was observed without the addition of 2D-DWT coefficients, the achieved accuracy is 95.3%, and AUC is 0.99. The confusion matrix and AUC are illustrated in Fig. 6. Thus, it shows that the accuracy is increased from 95.3% to 99.3%, i.e., 4%, by adding 2D-DWT coefficients.

5. Conclusion

In this paper, we described a hybrid model which uses the high-level deep features of AlexNet and coefficients of 2D-DWT. The generated features were concatenated to build a combined set of features. The integrated high-level features set fed to SVM for classification of three kinds of lung histopathological images. We used the histopathological images of the LC25000 dataset to train and validate our method. The achieved accuracy indemnifies with a 99.3% classification accuracy, the model is highly reliable for lung cancer identification. Again, the comparative analysis is carried out with other machine learning and deep learning models; it implies that the proposed method outperformed to others. This research helps design a computer-based diagnosis system for identifying lung cancer, reducing pathologists' effort, cost, and time.

References

[1] Cancer Key Facts, https://www.who.int/news-room/fact-sheets/detail/cancer. Last accessed 25 Aug 2020
[2] F. Melani and L. Bruzzone, Classification of hyperspectral remote sensing images with support vector machines, *IEEE Trans. Geosci. Remote Sens.* **42** (2004), 1778–1790.
[3] Y. Wang and H. Duan, Classification of hyperspectral images by SVM using a composite kernel by employing spectral, spatial and hierarchical structure information, *Remote Sens.* **10** (2018), 441.
[4] F. Ratle, G. Camps-Valls and J. Weston, Semisupervised neural networks for efficient hyperspectral image classification, *IEEE Trans. Geosci. Remote Sens.* **48** (2010), 2271–2282.
[5] Y. Chen, N.M. Nasrabadi and T.D. Tran, Hyperspectral image classification via kernel sparse representation, *IEEE Trans. Geosci. Remote Sens.* **51** (2013), 217–231.
[6] J. Ham, Y. Chen, M.M. Crawford and J. Ghosh, Investigation of the random forest framework for classification of hyperspectral data, *IEEE Trans. Geosci. Remote Sens.* **43** (2005), 492.
[7] Y. Hou, Breast cancer pathological image classification based on deep learning, *J Xray Sci Technol.* **28**(4) (2020), 727–738.
[8] Y. Yang and C. Guan, Classification of histopathological images of breast cancer using an improved convolutional neural network model, *J Xray Sci Technol.* **30**(1) (2022), 33–44.
[9] J. Schmidhuber, Deep learning in neural networks: An overview, *Neural Netw.* **61** (2015), 85–117.
[10] A.R. Sanjay, R. Soundrapandiyan, M. Karuppiah and R. Ganapathy, CT and MRI image fusion based on discrete wavelet transform and type-2 fuzzy logic, *International Journal of Intelligent Engineering and Systems* **10**(3) (2017), 355–362.
[11] J. Sun, X. Cai, F. Sun and J. Zhang, Scene image classification method based on Alex-Net model, *2016 3rd International Conference on Informative and Cybernetics for Computational Social Systems (ICCSS)* (2016), 363–367.
[12] L.B. Lusted, Medical electronics, *N. Engl. J. Med.* **252** (1955), 580–585.
[13] G.S. Lodwick, T.E. Keats and J.P. Dorst, The coding of roentgen images for computer analysis as applied to lung cancer, *Radiology* **81** (1963), 185–200.
[14] R. Thawani, M. McLane, N. Beig, et al., Radiomics, and radiogenomics in lung cancer: A review for the clinician, *Lung Cancer* **115** (2018), 34–41.
[15] Y. Xu, L. Jiao, S. Wang, et al., Multi-label classification for colon cancer using histopathological images, *Microsc. Res. Tech.* **76** (2013), 1266–1277.
[16] J. Kuruvilla and K. Gunavathi, Lung cancer classification using neural networks for CT images, *Comput. Methods Programs Biomed.* **113** (2014), 202–209.
[17] S.A. Deppen, J.D. Blume, C.D. Kensinger, et al., Accuracy of FDG-PET to diagnose lung cancer in areas with infectious lung disease: A meta-analysis, *JAMA J. Am. Med. Assoc.* **312** (2014), 1227–1236.
[18] W. Shen, M. Zhou, F. Yang, et al., Multi-crop Convolutional Neural Networks for lung nodule malignancy suspiciousness classification, *Pattern Recognit.* **61** (2017), 663–673.
[19] W. Sun, B. Zheng and W. Qian, Automatic feature learning using multichannel ROI based on deep structured algorithms for computerized lung cancer diagnosis, *Comput. Biol. Med.* **89** (2017), 530–539.
[20] Z. Yuan, M. Izady Yazdanabadi, D. Mokkapati, et al., Automatic polyp detection in colonoscopy videos, *Med. Imaging 2017 Image Process*. (2017), 101332K.

[21] R. Selvanambi, J. Natarajan, M. Karuppiah, et al., Lung cancer prediction using higher-order recurrent neural network based on glowworm swarm optimization, *Neural Comput. Appl.* **32** (2020), 4373–4386.
[22] A.O. de Carvalho Filho, A.C. Silva, A.C. de Paiva, et al., Classification of patterns of benignity and malignancy based on CT using topology-based phylogenetic diversity index and convolutional neural network, *Pattern Recognit.* **81** (2018), 200–212.
[23] R.V.M. da Nóbrega, P.P. Rebouças Filho, M.B. Rodrigues, et al., Lung nodule malignancy classification in chest computed tomography images using transfer learning and convolutional neural networks, *Neural Comput. Appl.* **32** (2020), 11065–11082.
[24] H.Y. Chiu, H.S. Chao and Y.M. Chen, Application of artificial intelligence in lung cancer, *Cancers* **14**(6) (2022), 1370.
[25] S. Mehmood, T.M. Ghazal, M.A. Khan, et al., Malignancy detection in lung and colon histopathology images using transfer learning with class selective image processing, *IEEE Access* **10** (2022), 25657–25668.
[26] N. Kumar, M. Sharma, V.P. Singh, et al., An empirical study of handcrafted and dense feature extraction techniques for lung and colon cancer classification from histopathological images, *Biomedical Signal Processing and Control* **75** (2022), 103596.
[27] S. Tomassini, N. Falcionelli, P. Sernani, et al., Lung nodule diagnosis and cancer histology classification from computed tomography data by convolutional neural networks: A survey, *Computers in Biology and Medicine* (2022), 105691.
[28] Y. Chen, H. Yang, Z. Cheng, et al., A whole-slide image (WSI)-based immunohistochemical feature prediction system improves the subtyping of lung cancer, *Lung Cancer* **165** (2022), 18–27.
[29] G.A. Kassis, M.R. Makowski, D. Rückert, et al., Secure, privacy-preserving and federated machine learning in medical imaging, *Nat Mach Intell* **2** (2020), 305–311.
[30] L. Alzubaidi, M.A. Fadhel, O. Al-Shamma, et al., Towards a better understanding of transfer learning for medical imaging: a case study, *Applied Sciences* **10**(13) (2020), 4523.
[31] B.K. Natural and H.C. Thapa, Lung cancer detection using convolutional neural network on histopathological images, *International Journal of Computer Trends and Technology* **68**(10) (2020), 21–24.
[32] S. Mangal, A. Chaurasia and A. Khajanchi, Convolution neural networks for diagnosing colon and lung cancer histopathological images. arXiv preprint, 2020, arXiv:2009.03878.
[33] Y. Shi, Y. Gao, Y. Yang, et al., Multimodal sparse representation-based classification for lung needle biopsy images, *IEEE Trans. Biomed. Eng.* **60** (2013), 2675–2685.
[34] J. Kuruvilla and K. Gunavathi, Lung cancer classification using neural networks for CT images, *Comput. Methods Programs Biomed.* **113** (2014), 202–209.
[35] A. Masood, B. Sheng, P. Li, et al., Computer-assisted decision support system in pulmonary cancer detection and stage classification on CT images, *J. Biomed. Inform.* **79** (2018), 117–128.
[36] P.M. Shakeel, A. Tolba, Z. Al-Makhadmeh and M.M. Jaber, Automatic detection of lung cancer from biomedical data set using discrete AdaBoost optimized ensemble learning generalized neural networks, *Neural Comput. Appl.* **32** (2020), 777–790.
[37] S. Suresh and S. Mohan, ROI-based feature learning for efficient true positive prediction using convolutional neural network for lung cancer diagnosis, *Neural Comput. Appl.* **32** (2020), 15989–16009.
[38] M. Masud, G. Muhammad, M.S. Hossain, et al., Light deep model for pulmonary nodule detection from CT scan images for mobile devices, *Wirel. Commun. Mob. Comput.* (2020), 8893494.
[39] P.M. Shakeel, M.A. Burhanuddin and M.I. Desa, Automatic lung cancer detection from CT image using improved deep neural network and ensemble classifier, *Neural Comput. Appl.* **34** (2020), 9579–9592.